Journal of Power Sources, 47 (1993) 129–147

Investigations of the negative plate of lead/acid cells 1. Selection of additives

Michel Saakes, Pieter J. van Duin, Alexander C.P. Ligtvoet and Dick Schmal
TNO Environmental and Energy Research, P.O. Box 6011, 2600 JA Delft (Netherlands)

(Received October 16, 1992; accepted July 12, 1993)

Abstract

A procedure is proposed for the selection of inhibitors and expanders used as additives for the negative plate of the lead/acid battery. Inhibitors were selected by performing d.c. and a.c. measurements at pure metals (Cu, Sb, Ag), which are assumed to act as local active sites for the hydrogen-evolution reaction at the negative plate. From this study anisaldehyde was found to show strong preferential adsorption at Cu and Sb. Expanders were selected using a.c. impedance measurements at a Pb electrode at a low anodic discharge current. Selected expanders were Indulin C and Na-1-naphtol-4-sulfonate. From the impedance measurements information was obtained not only on the expander action but also on the effect of the additive on the double layer and the diffusion properties of lead sulfate. From a study on the concentration dependence of the expander (Na-1-naphtol-4-sulfonate) an optimal effect was found at a concentration of about 600 ppm.

Introduction

Since the early start of manufacturing lead/acid cells, the use of additives, and more specifically the selection of these compounds, has been guided by empirical rules and experience. During the last decades the lead/acid cell has been the subject of many studies, which have increased enormously the knowledge of the effects of additives and of the manufacturing process.

Despite this, the need was felt to develop a systematic procedure for the selection of two of the more important types of additives, viz., inhibitors (for suppression of hydrogen evolution) and expanders (for maintaining the active surface area/pore structure of the active material).

In part 1 of this series of two papers, the selection procedure is described and elucidated with d.c. and a.c. voltammetry tests on small, smooth electrodes. Part 2 describes tests in 2 V laboratory lead/acid cells as well in a practical cell with commercial negative (and positive) plate materials and gives conclusions about the applicability of the selection procedure [1].

Background information

The main types of additives are inhibitors and expanders. From the many additives found in the literature some 20 compounds have been selected for a quantitative study on their inhibitor and/or expander properties.

Inhibitor action

Hydrogen-evolution reaction

The voltage of a charged lead/acid cell, at the end of the charging process, is built up by three components: oxygen overvoltage at the positive plate, hydrogen

overvoltage at the negative plate and ohmic drop due to the limited conductivity of electrolyte and grid. The significance of a high overvoltage for the hydrogen-evolution reaction (HER) can be understood when considering the main reaction at the negative plate, i.e., reduction of lead sulfate to lead. The driving force for the reduction of lead sulfate to lead is by the potential. Due to the high overvoltage for the HER at lead, the negative plate is kinetically stable and lead sulfate can be reduced to lead with a high coulomb efficiency.

However, the high overvoltage for the HER at lead, is gradually lowered during the cycle life of the lead/acid cell. This decrease in overvoltage is caused by the deposition of foreign metals, with a lower overvoltage for the HER on the negative plate originating from corrosion processes at the positive grid.

These metals are Sb, Cu and/or Ag. Sb is used for the positive grid as an alloy element to improve the casting properties. Cu is generally present in small amounts. These foreign metals exhibit a strong poisoning effect on the negative plate because of their catalytic effect on the HER. The ideal inhibitor should block selectively the active sites by preferential adsorption. The purpose of this paper is to investigate the existence of such compounds and the extent to which they block these active sites, without exerting a negative influence on the cell properties.

We, therefore, made measurements at the pure metals that are believed to be involved in active hydrogen-evolution sites.

Adsorption at pure metals and the potential of zero charge

One possibility to overcome the effect of active sites at the negative plate is to block these sites by adding compounds which adsorb selectively at these sites.

Adsorption of compounds at the electrode/electrolyte interface is governed by, at least, two important factors: (i) electrostatic forces (attraction, repulsion), and (ii) specific chemical interactions.

The first factor is determined by the sign and the magnitude of the surface charge. The surface charge can be obtained once the differential double-layer capacitance and the potential of zero charge are known. However, if the double-layer capacitance is not available, only the sign of the surface charge can be determined if the potential of zero charge is known.

In Fig. 1 the potential of zero charge, E_{pzc}, is given for Pb [2], Cu [3], Sb [2, 4] and Ag [4]. This Fig. gives the working potential range of the negative plate which allows determination of the sign of the different metal surfaces.

As can be seen, the surface charge at Cu is always negative while for Ag and Pb it is always positive, independent of the potential of the negative plate in the indicated range ΔE. This difference shows up the possibility of using selective adsorption applying electrostatic arguments only. The sign of the Sb surface depends on the state-

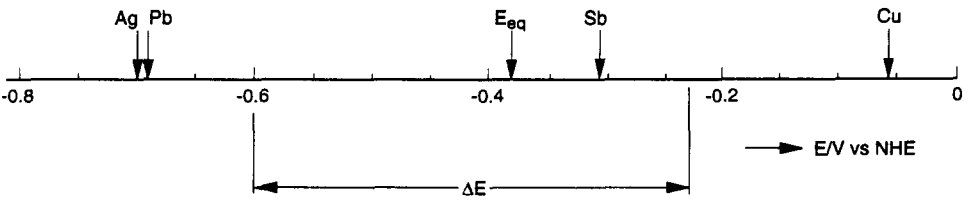

Fig. 1. Potential of zero charge for Pb, Cu, Sb and Ag. The working potential range of the negative plate is indicated by ΔE. The value of E_{eq} is the equilibrium potential of the lead/lead sulfate couple.

of-charge of the negative plate. In the HER potential region, the Sb surface is charged negatively.

From Fig. 1 we conclude that in the HER potential region, both Cu and Sb are charged negatively, while Pb and Ag are charged positively.

Hydrogen evolution at the equilibrium potential

When no external current is present, still hydrogen gas is evolved from the lead/acid cell (self-discharge reaction at the negative plate) because under normal conditions E_{eq} is more negative than the HER equilibrium potential, the difference being the overvoltage of the HER. The rate of this self-discharge process is determined by the rate of the reduction of hydrogen ions to hydrogen gas since the oxidation process of lead to lead ions is fully reversible. In Fig. 2 the self-discharge process is presented.

In the presence of an active site (Me = Cu, Sb or Ag), the rate of self-discharge is accelerated. Because the self-discharge process is always operative, eventually all of the lead present will be converted to lead sulfate. The rate of self-discharge is expressed in a progressive loss in capacity (Ah) per day. For commercial lead/acid cells, this loss is less than 0.1% per day. An increase of this value is highly undesirable and the addition of selective inhibitors is therefore also important to keep the self-discharge rate low.

Expander action

Expanders are added to the negative plate during manufacture to affect the crystallization processes that take place during charging and discharging of the cell. Some of these compounds also show inhibitor action. Table 1 gives a survey of some 14 expanders, 4 of them studied by us. They are: Vanisperse A, Reax 80C, Indulin C and Na-1-naphtol-4-sulfonate.

The action of expanders is explained by the adsorption of the expander at lead and lead sulfate crystals.

First, we consider the influence on the lead sulfate crystallization. The adsorption at lead sulfate crystals decreases the crystallization rate which results in the formation of more and therefore smaller crystals. This decrease in size of the lead sulfate crystals has a beneficial effect on the capacity of the negative plate. The rate of crystallization, k, can be determined by impedance measurements from which the crystallization resistance $R_k \sim 1/k$ is obtained.

During charging the expander can also affect the deposition process of lead during the formation of the lead lattice. If the expander shows adsorption at lead crystals, the porosity of the lead lattice formed will be larger. Adsorption of the expander is deduced from the value of the differential double-layer capacitance, C_d, of the lead/lead sulfate, sulfuric acid interface.

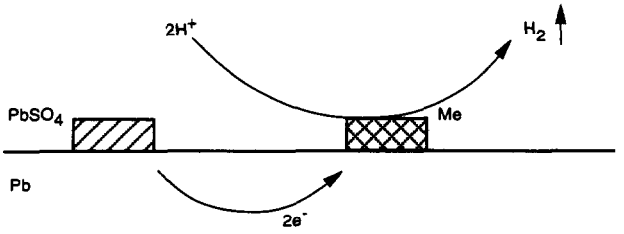

Fig. 2. Schematic mechanism of self-discharge at the negative plate in the presence of an active site (Me).

TABLE 1

Survey of expanders for the negative plate

Expander	Description	Reference
Ca-ligninsulfonate	wood product	5
Oxylignin	wood product	5
Indulin C	wood product	6, this work
Na-humic acid	wood product	5
Totanin FNA	wood product	7
Vanisperse A	wood product	8, this work
BNF	polycondensation product of phenol and β-naphtol-sulfonic acid	9–13
$CoSO_4$	inorganic salt	14
Reax 80C	wood product	15, 16, this work
DSV	desulfonated high molecular fraction of vanillin production	17
SUNIL	sulfonated nitrolignin	11
1-Naphtol-4-sulfonic acid	aromatic sulfonic acid	17, this work
α-Naphtol	aromatic hydroxide	4, 17
α-ONK	alpha-oxynaphthoic acid	4

A quantitative comparison of the action of the studied expanders will be given in the section describing the impedance measurements.

Selection procedure

Additives have been tested by means of the selection procedure described below. Small electrodes of pure metals were used, simulating local active sites at the negative plate.

The measurement techniques used are d.c. voltammetry in the potential range of the HER (inhibitors), a.c. voltammetry (impedance measurements) in the frequency range 10–3000 Hz and at a small anodic discharge current density (40 μA cm^{-2}) and cycling tests with commercial plate materials.

In Table 2 the selection procedure is given. The sequence in Table 2 has been obtained gradually on the basis of a number of years of experience with inhibitor/expander research. Impedance measurements of the lead/lead sulfate system in sulfuric acid and absorption properties are preferentially made at smooth electrodes. The use of porous electrodes for these measurements severely troubles the analysis because then also geometrical parameters are involved. In part 2 the results obtained at smooth electrodes are tested in cycling tests with commercial plate materials [1].

Experimental part

D.c. voltammetry

D.c. measurements were taken by means of a voltage scan generator (model VSG72, Bank), standard potentiostat (model ST72, Bank) and an *x-y* recorder (model PM8120, Philips). Scan rate was 0.5 mV s^{-1}.

TABLE 2

Selection procedure for additives

Sequence	Remarks
Preliminary selection	Literature information electrode potential applied potential type of electrolyte electrolyte concentration Availability Solubility in sulfuric acid Stability in sulfuric acid
Adsorption studies via measurements of direct current (d.c. measurements) double-layer capacitance (C_d)	Electrode material Electrode potential Electrolyte concentration Temperature Concentration of additive
Impedance of the $Pb/PbSO_4$, H_2SO_4 interface (a.c. measurements)	Charge-transfer resistance Crystallization resistance Double-layer capacitance Warburg impedance
Stability	Oxidation at PbO_2
Test in 2 V laboratory cell	Concentration needed Lifetime of additive Influence on hydrogen overvoltage capacity charge/discharge behaviour lifetime of cell temperature range of cell
Verification in a practical cell or battery	Method of addition Safety Price Temperature

A.c. voltammetry

Lock-in-amplifier setup

Differential double-layer measurements were taken using a lock-in-amplifier (LIA) model 129A, PAR), a sine wave generator (model 185, Wavetek), a standard potentiostat (model ST72, Bank) and a voltage scan generator (model VSG72, Bank). In-phase and quadrature components were recorded on *x-t* recorders (model BD40, Bank) and read out by digital multimeters (model 3478A, HP). The a.c. measurements were performed in a frequency range of 20 to 2000 Hz.

Measurements with this system were done using a three-electrode configuration (Me working electrode (Me = Pb, Cu, Sb), Pt counter electrode and saturatel calomel (SCE) reference electrode). The a.c. measurements on the effect of some expanders (cf., Table 7) were done with the LIA set-up.

Frequency response analyser setup

A.c. impedance measurements, on the concentration effect of Na-1-naphtol-4-sulfonate (cf., Table 8), on the system $Pb/PbSO_4$, H_2SO_4, were made using a frequency

response analyzer system (AUTOLAB PGSTAT20) developed by Ecochemie in co-operation with TNO (The Netherlands).

The accuracy of the FRA system was improved by time domain averaging (1 to 4096) and by soft-ware controllable amplifiers and programmable filters (1 Hz to 140 kHz). The sampling rate could be varied from 0.2 Hz to 200 kHz. The accuracy obtained for the amplitude was 0.1 dB at 10 kHz and for the phaseshift 0.2 degrees at 10 kHz with 1 kΩ source resistance. The dynamic range was 0.1 to 10^9 Ω. The signal generator used had an output amplitude of 1–500 mV and a maximum number of points per cycle of 65 536 (16-bit DAC).

Measurements with this system, using a two-electrode configuration (Pb working electrode and Pt counter electrode) were limited to 10–3000 Hz in practice. The reason for this was the potential of the counter electrode which is not well defined. This resulted in a poor resolution (about 1%) of the a.c. potential of the measured impedance since the d.c. potential could not be substracted properly. This problem was overcome by introducing a large value electrolytic capacitor (1000 μF) connected in series with the working electrode. Using this capacitor, high accuracy impedance measurements could be made in a restricted frequency range of 10–3000 Hz. For the system under study, this frequency range appeared to be sufficient.

Impedance measurements, made at a small anodic current density (40 μA cm^{-2}), were achieved with maximum accuracy if the a.c. current was, at every frequency, given such value that the a.c. voltage was equal to about 5 mV. Before every frequency, the Pb electrode was equilibrated 10 s at a low discharge current before sampling was done for 20 s.

Electrode preparation

For Pt, Pb and Cu electrodes, chemical cleaning methods were used.

In the case of Pt, used as counter electrode, a mixture of nitric acid and hydrochloric acid was used.

In the case of Pb, etching was done with a mixture of 80 vol.% 100% acetic acid and 20 vol.% 30% hydrogen peroxide. Cleaning was done by shaking the electrode for approximately 10 s. Afterwards, the electrode was rinsed with bi-distilled water. This procedure was repeated until the electrode appeared shiny.

In the case of Cu, etching was done in a warm mixture (1:1:1) of concentrated nitric acid, phosphoric acid and acetic acid. Shaking was done for some seconds, followed directly by rinsing with bi-distilled water.

In the case of Sb, electrodes were made by melting Sb bars in a quartz tube in an electrical furnace, followed by slow cooling. After breaking the glass, a smooth surface was obtained.

In the case of Ag, a lead electrode was plated with Ag by applying a cathodic current in a 50 ppm Ag^+ solution.

After cleaning, the electrodes (Pb, Cu, Sb, and Ag) were first exposed to a cathodic current in order to reduce any oxides present.

Electrode and cell dimensions

The working electrode (1.3 cm^2) (Pb, Cu, Sb, and Ag) had a cylindrical shape (diameter: 0.2 cm, length: 2 cm) and was soldered to a tinned copper wire. The electrical connection was isolated using acid-resistant polymer tubing.

The counter electrode (Pt) was a cylindrical sheet (total area (both sides): 72 cm^2).

The reference electrode was a commercial SCE connected to the cell using a salt bridge.

The cell was a H-type cell with two compartments connected by a porous glass. The cell compartments were connected to a nitrogen atmosphere. The working compartment was purged with nitrogen gas.

Measurement conditions

All measurements were made at room temperature (≈20 °C). Solutions were prepared with bi-distilled water and p.a. reagents or the highest quality available. The metals, Pb, Cu and Sb, had a 99.999% purity grade.

Results

Inhibitors

Hydrogen evolution at pure metals in H_2SO_4

In order to compare quantitatively the differences of overvoltage for the HER, Tafel plots were made by plotting semi logarithmically the measured faradaic current for the hydrogen-ion reduction versus the applied potential. Figure 3 shows the Tafel plots for Pb, Cu and Sb.

Fore a more systematic study of the HER for various metals reference is made to Vetter [18]. From Fig. 3 we conclude that both Cu and Sb strongly enhance the

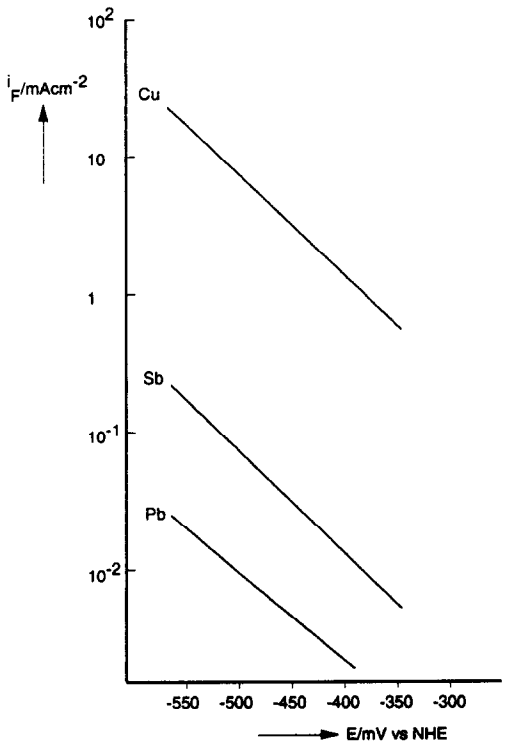

Fig. 3. Tafel plots for Pb, Cu and Sb.

hydrogen evolution. Cu, for example, which is present to a lesser extent than Sb, has a drastic effect on the HER by increasing the faradaic current approximately by three orders of magnitude.

Hydrogen evolution in the presence of additives

Copper. The HER at Cu was studied at two potential, i.e., −0.8 and −0.7 V versus SCE (−0.56 and −0.46 V versus NHE, respectively). At these potentials, the faradaic current density, i_{dc}, was measured in the presence of some 18 additives at a concentration of 200 ppm. The differential double-layer capacitance, C_d, measured at −0.7 V versus SCE, was obtained from the slope of $Y''/\sqrt{\omega}$ versus $\sqrt{\omega}$ ($\omega = 2\pi f$, where f is the a.c. frequency) assuming no surface roughness and irreversible hydrogen reduction. The values of i_{dc} and C_d are given in Table 3.

The compounds in Table 3 are listed in order of decreasing value of i_{dc}, measured at −0.8 V versus SCE.

From Table 3 it follows that anisaldehyde almost completely blocks the HER at Cu. Compared with the blank case, the value of i_{dc} decreased (after equilibration) with a factor 680, which makes its value almost equal to pure lead. Other compounds, presented in Table 3, with an aldehyde group, both aliphatic and aromatic, also show a strong adsorption at Cu. Examples include: hexanal, benzaldehyde and salicylaldehyde.

TABLE 3

Values of i_{dc} and C_d at copper in 5.2 M H_2SO_4 for 18 additives (concentration: 200 ppm). Potentials refer to a SCE reference electrode

Additive	i_{dc} (mA cm^{-2}) (−0.8 V)	i_{dc} (mA cm^{-2}) (−0.7 V)	C_d (μF cm^{-2}) (−0.7 V)
None	19.1	3.5	17.6
Phenol-4-sulfonic-acid	48.9	10.1	21.5
Benzotriazole	38.0	5.8	18.2
Reax 80C [a]	20.5	2.3	6.5
Isonicotinaldehyde	18.6	2.5	27.8
4-Hydroxyquinoline	17.1	2.3	23.0
1,10-Phenanthroline	15.5	2.2	24.6
$TBABF_4$ [b]	15.1	2.8	8.9
ENSA-6 [c]	13.7	2.1	6.9
Anthranilic acid	12.4	1.4	15.9
Thiourea	11.6	0.66	18.2
Isonicotinic acid	10.9	1.8	21.4
2,3,5-Triphenyl-tetrazolium chloride	9.3	0.53	18.8
3-Hydroxybenzaldehyde	9.2	1.2	5.5
Benzaldehyde	3.8	1.2	3.3
Hyamine 2389 [d]	1.5	0.07	9.0
Hexanal	0.43	0.18	1.9
Salicylaldehyde	0.11	0.016	1.1
Anisaldehyde	0.028	0.012	0.4

[a]Sulfonated wood compound (Westvaco Inc.).
[b]Tetrabutylammoniumtetrafluoborate.
[c]Naphthalene sulfonic acid, substituted with predominantly six ethoxy groups.
[d]Cationic surfactant with methyl-dodecyl-benzyl-trimethyl ammonium chloride and methyl-dodecylxylylene-bistrimethyl ammonium chloride (BDH chemicals, Ltd.)

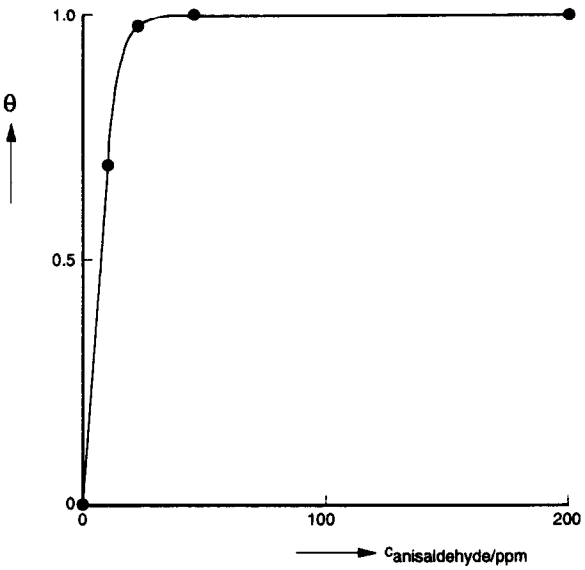

Fig. 4. Adsorption isotherm for the adsorption of anisaldehyde at copper, at −0.7 V vs. SCE, in 5.2 M sulfuric acid.

The applicability of anisaldehyde and other compounds showing inhibitor activity will be guided, however, also by their effects on other processes occurring in the lead/acid cell as will be discussed further on.

The concentration dependence of the adsorption of anisaldehyde, which was selected from Table 3 because of its strongest inhibitor action, was investigated. Using a.c. impedance, the differential double-layer capacitance, C_d, was measured to obtain the fractional surface coverage θ equal to:

$$\theta = (C_d^0 - C_d)/(C_d^0 - C_d^1) \quad (1)$$

where C_d^0 and C_d^1 are equal to the value of C_d without an additive present (blank) and in case of a saturated solution with an additive. Equation (1) holds only if $d\theta/dE \approx 0$, that is when the potential dependence of the surface coverage is negligible.

Figure 4 shows the adsorption isotherm for anisaldehyde at Cu in 5.2 M sulfuric acid.

From Fig. 4 we conclude that the surface coverage is complete at a concentration of ~20 ppm. This low saturation concentration is favourable for a possible application. A simple method to detect concentrations of anisaldehyde below 20 ppm is UV spectroscopy. Figure 5 shows the absorption spectrum for 1 ppm level in cyclohexane.

Using the adsorption peaks, an easy and sensitive detection is possible. Should more UV absorbing species be present, detection at more wavelengths becomes necessary.

Antimony. Figure 3 shows that Sb increases the HER approximately by a factor of six, compared with Pb. Although the rate of the HER at Sb is much lower than at Cu, the larger amount of Sb present in the positive grid and, due to corrosion, deposited on the negative plate, can lead to a significant decrease in charge efficiency of the cell.

Possible inhibitors for the HER at Sb were selected from the literature and are given in Table 4.

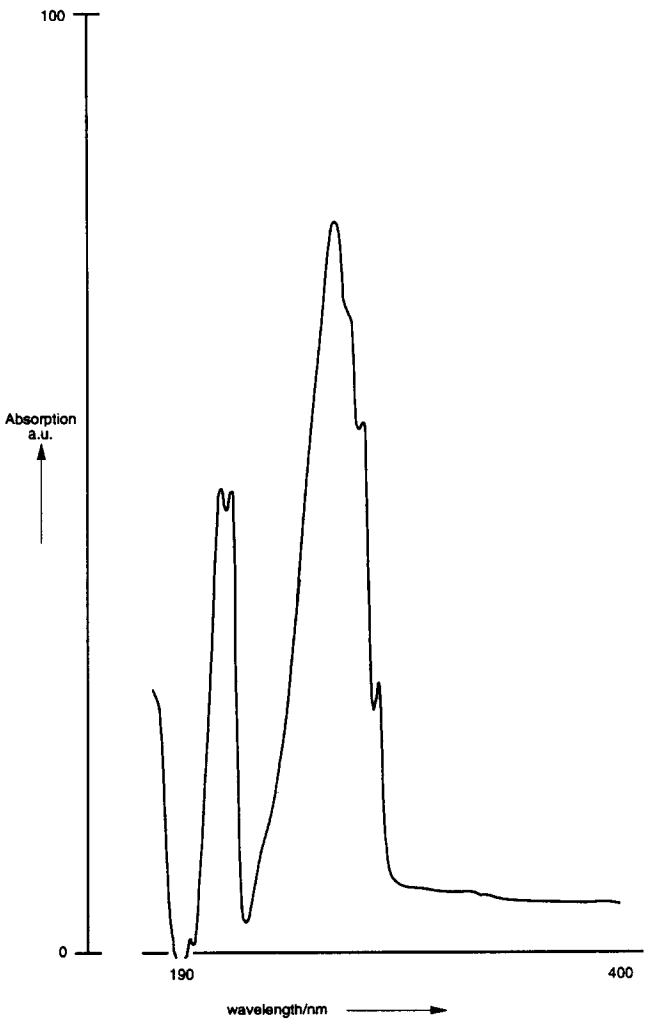

Fig. 5. UV absorption spectrum of 1 ppm anisaldehyde in cyclohexane.

Both at Cu and Sb, the HER is inhibited by substituted benzaldehydes. Both metals are charged negatively in the potential range of the negative plate where hydrogen gas is evolved.

One striking difference between Cu and Sb is that Sb is able to form a hydride SbH_3 (stibine) at negative potentials. This hydride is a poisonous gas evolved during charge [22]. During overcharge, stibine is formed at the negative plate and removes the Sb present. However, since the formation of Sb(III) at the positive plate, due to corrosion, is a continuous process, there will always be Sb present at the negative plate.

Silver. The additives were tested at a concentration of 30 ppm. In Table 5 the results are given. Especially α-naphtol shows strong inhibitor action. However, at a somewhat higher concentration (50 ppm), we found that α-naphtol strongly passivated

TABLE 4

Inhibitors for the HER at antimony found in the literature

Additive		Reference
Benzaldehyde		
2-hydroxy-	(salicylaldehyde)	2
4-hydroxy-		2
3-methoxy-4-hydroxy-	(vanillin)	2
2-methoxy-		19
4-methoxy-	(anisaldehyde)	20, 21
Acetophenon		
2,6-dihydroxy		2
Benzene		
1,2-dihydroxy-	(catechol)	20
1-hydroxy-2-methoxy-	(guaiacol)	20

TABLE 5

Effect of some additives on the HER at silver at −0.8 V vs. NHE (concentration: 30 ppm)

Additive	$i_{additive}/i_{blank}$
None	1
1-Naphtol-4-sulfonic acid	0.38
Humic acid	0.22
1-Hydroxy-4-sulfonic acid	0.20
Ferulic acid	0.18
Reax 80C	0.13
α-Naphtol	0.10

the surface of Pb, which resulted in a drastic decrease of the discharge capacity. The inhibitor action of Reax 80C and 1-naphtol-4-sulfonic acid is interesting because these compounds also show expander action. This illustrates that a compound's action can be manifold.

Besides inhibition, also acceleration of the HER at Ag is possible. In the case of 100 ppm benzotriazole, the faradaic current was 1.6 times the value in the absence of this additive.

We conclude that inhibition of the HER at Ag is feasible with compounds which are already present in the system as expanders, for example Reax 80C and 1-naphtol-4-sulfonic acid.

The effect of Reax 80C at Ag is in contrast to that on Cu, where no inhibitor action was found (Table 3). The inhibiting effect both at Pb and Ag for Reax 80C can possibly be explained by the same sign of the charge at the surface of Ag and Pb, both metals having almost the same value for E_{pzc} (Fig. 1).

Lead. Preferably, the lead surface that is not contaminated with Cu, Sb and Ag should adsorb as little additive as possible, so that the used amount of additive can be kept small. In the ideal case, the additive shows only adsorption at places where

TABLE 6

Values of i_{dc} (μA cm^{-2}) and C_d (μF cm^{-2}) for some inhibitors for the HER at lead. Potentials refer to a SCE reference electrode

Additive	Code Fig. 6	i_{dc} (−0.8 V)	C_d (−0.8 V)	i_{dc} (−0.7 V)	C_d (−0.7 V)
None	a	22.1	21.3	4.5	25.3
Reax 80C	b	19.4	15.5	8.5	17.9
Benzaldehyde	c	13.2	8.9	10.1	20.4
3-Hydroxybenzaldehyde	d	19.4	11.1	9.3	12.4
Salicylaldehyde	e	10.0	4.0	6.2	4.8
Anisaldehyde	f	14.8	7.8	15.5	11.9
Benzotriazole	g	16.3	24.9	4.7	29.7

the HER is accelerated. Because such ideal additives are not available, a compromise exists of using additives that show (strong) preferential adsorption at active sites.

Studies of adsorption at Cu and Sb showed that both anisaldehyde and salicylaldehyde give (strong) adsorption. Therefore, we studied also their adsorption behaviour at Pb to find out whether this adsorption behaviour is specific for Cu and Sb only.

In Table 6 values of i_{dc} and C_d are given for two potentials (−0.7 and −0.8 V versus SCE). The concentration of the additive was 200 ppm.

From Table 6 we conclude that anisaldehyde shows only weak adsorption at Pb. This means that anisaldehyde can be used to cover Cu in a selective way.

Salicylaldehyde, which showed strong adsorption at Cu and Sb, is found to give moderate adsorption at Pb, which makes a possible application less favourable.

Reax 80C, used as an expander, shows almost no adsorption at Pb.

The use of 3-hydroxybenzaldehyde is, in contrast with 2-hydroxybenzaldehyde (salicylaldehyde), limited by poor stability in sulfuric acid. After some weeks it was degraded, leaving behind a black deposit.

In Fig. 6 it is seen that most of the compounds show a linear relationship between the suppression of the HER and the differential double-layer capacitance.

From the additives investigated, benzotriazole behaves differently. At −0.8 V versus SCE, the value of i_{dc} decreased somewhat at an increased value of C_d compared with the blank case.

Expanders

Expander action was investigated by means of electrochemical impedance spectroscopy. First a selection was made between the action of some expanders. The frequency range measured was 20–1020 Hz using the LIA setup.

In case the charge-transfer resistance, R_F, for the oxidation of lead to lead ions can be neglected, the analysis of the electrode admittance Y_e (Y_e is the value of Y corrected for the ohmic resistance) is done following the equations derived before in refs. 9, 10–14, 23 and 24:

$$Y_e' = \frac{1}{R_k} + \frac{\sqrt{\omega}}{A\sqrt{2}} \tag{2}$$

$$\frac{Y_e''}{\sqrt{\omega}} = \frac{1}{A\sqrt{2}} + C_d\sqrt{\omega} \tag{3}$$

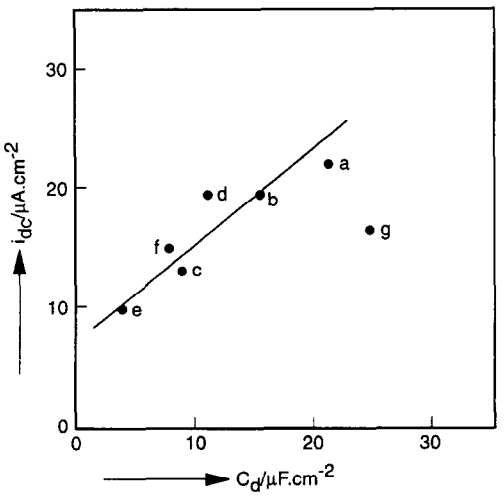

Fig. 6. Correlation between i_{dc} and C_d for some additives at lead at -0.8 V vs. SCE (concentration: 200 ppm).

where Y_e' and Y_e'' are the real and imaginary component of the electrode admittance, ω is the angular frequency ($\omega = 2\pi f$) and $A = RT/(n^2F^2c_0D^{1/2})$ (c_0 is the equilibrium concentration of lead sulfate).

If, however, passivation of lead is present, R_F can no longer be neglected and eqns. (2) and (3) are no longer valid. For that case an analysis procedure is given in the Appendix for deriving the parameters R_F, R_k, C_d and A using two linear equations.

In Fig. 7 the effect of some expanders on the impedance of the system $Pb/PbSO_4$, H_2SO_4 is given by the complex impedance representation. The expander concentration used was 200 ppm.

Table 7 shows the values of the parameters R_k, C_d and A including the margin of error obtained from the linear fits according to eqns. (2) and (3). Table 7 gives also the parameters for BNF, an expander studied in refs. 9–13.

It must be emphasized that the expander action depends on the concentration used. Therefore, the values in Table 7 are only indicative.

From Table 7 it follows that Indulin C, at a concentration of 200 ppm, has the largest effect on the crystallization resistance R_k. Compared with the blank case, the rate of crystallization of lead sulfate is approximately three times lower. This results in the formation of smaller lead sulfate crystals during discharge and a higher porosity during charge. The effect on a macroscale is the increase of charge and discharge capacity of the negative plate.

From the values of C_d given in Table 7 we conclude that the expanders studied give mostly weak adsorption. BNF (saturated solution) shows the highest effect on the differential double-layer value.

The parameter A ($\sim 1/\sqrt{D}$) has the largest value in case of BNF which is attributed to the formation of a diffusion barrier at the surface.

From Table 7, one expander, Na-1-naphtol-4-sulfonate, has been selected to study the effect of the concentration on the expander action (Fig. 8). As is already known, at high concentrations, severe adsorption can lead to the formation of a film, passivation of lead and sulfatation. At very low concentrations, the expander action will be (too) weak.

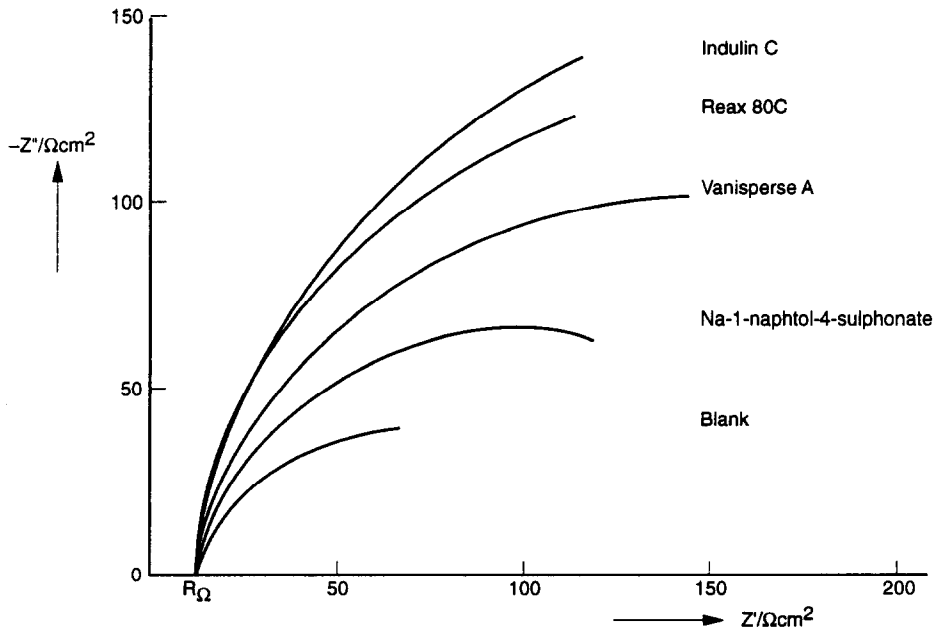

Fig. 7. Effect of some expanders on the impedance of the system lead/lead sulfate in 5.2 M sulfuric acid. The expander concentration was 200 ppm. The anodic discharge current was 40 μA cm^{-2}.

TABLE 7

Values of R_k, C_d and A for the system lead/lead sulfate, in 5.2 M sulfuric acid, derived from impedance measurements (LIA setup) at low anodic discharge current (40 μA cm^{-2})

Additive	Concentration (ppm)	R_k (Ω cm^{-2})	C_d (μF cm^{-2})	A (Ω cm^2 s$^{-1/2}$)
None		209 ± 17	35.0 ± 2.0	1384 ± 33
BNF saturated		662 ± 22	9.3 ± 0.3	9840 ± 527
Vanisperse A	200	382 ± 41	34.2 ± 4.3	3826 ± 128
Reax 80C	200	381 ± 27	23.5 ± 2.1	7424 ± 344
Indulin	200	698 ± 78	20.8 ± 0.9	5575 ± 171
Na-1-naphtol-4-sulfonate	200	279 ± 146	14.5 ± 0.2	2429 ± 131

The analysis was executed as before, using eqns. (2) and (3), assuming passivation of lead to be absent. In Table 8 the parameters R_k, C_d and A are given (including error margin) and the correlation coefficients r_1 and r_2 corresponding to eqns. (2) and (3), respectively. The high values of the correlation coefficients support the idea of the absence of lead passivation ($R_F \approx 0$).

It follows from Table 8 that, at increasing concentration of the additive, the value of C_d is lowered due to adsorption. The value of $A \sim 1/\sqrt{D}$ increases with increasing concentration of the additive because of a build-up of a diffusion barrier at the surface. The most interesting parameter is R_k, that has a maximum at 600 ppm.

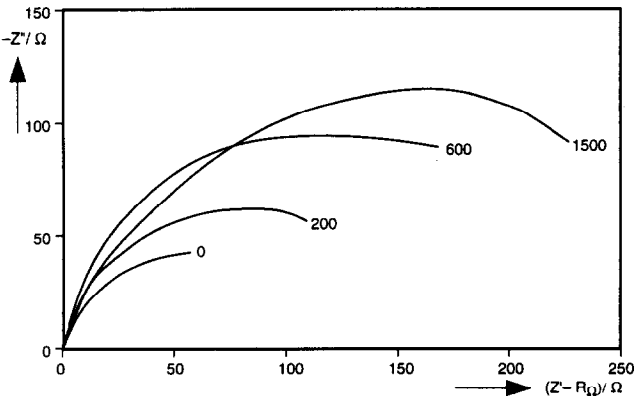

Fig. 8. Complex plane diagram for the system lead/lead sulfate for various concentrations of Na-1-naphtol-4-sulfonate in 5.2 M H_2SO_4; concentrations are indicated in ppm.

TABLE 8

Concentration dependence of the impedance parameters at different concentrations of Na-1-naphtol-4-sulfonate

Concentration (ppm)	C_d (μF cm^{-2})	R_k (Ω cm^2)	A (Ω cm^2 s$^{-1/2}$)	r_1	r_2
0	21.4 ± 0.5	334 ± 111	1448 ± 49	0.997	0.997
200	14.5 ± 0.2	279 ± 146	2429 ± 131	0.999	0.999
600	12.6 ± 0.2	962 ± 318	3425 ± 128	0.996	0.998
1500	5.7 ± 0.2	578 ± 130	4178 ± 207	0.993	0.994

Influence of anisaldehyde

In case an expander is added to restore the charge and discharge capacity of an aged cell or to improve the capacity of a newly-cycled cell, an increase of the HER reaction can decrease the cycling efficiency. In order to keep the cycling efficiency at a high value, beside an expander an inhibitor must be present. From the foregoing it was found that anisaldehyde shows preferential inhibitor action at active sites for the HER. From the a.c. measurements at a lead electrode, discharged at a low current density, it was shown that the action of an additive can be manifold. The influence of various concentrations of anisaldehyde on the discharge of lead to lead sulfate was therefore measured by a.c. impedance measurements to know whether anisaldehyde effects the discharge reaction. In Table 9, the physical parameters are given describing the discharge process using the eqns. (A3) and (A4) given in the Appendix. Measurements were done with the LIA setup. The parameters in the absence of anisaldehyde show some deviation from the blank case in Table 8. This is caused by another analysis that was used, another setup for obtaining the measurements and, inevitably, small differences in experimental conditions like surface state of the electrode and small impurities present. Both R_k and A are of the same order of magnitude as the values given in Table 8. Only C_d is somewhat higher.

From Table 9 we conclude that no significant influence is found on the crystallization resistance R_k. This means that anisaldehyde has no expander properties. Also the value of A does not change with varying concentration. From the decrease of C_d we

TABLE 9

Influence of anisaldehyde concentration on the discharge process of lead to lead sulfate

Concentration (ppm)	C_d (μF cm^{-2})	R_F (Ω cm^2)	R_k (Ω cm^2)	A (Ω cm^2 s$^{-1/2}$)
0	35	0 ± 3	177 ± 27	1783
22.5	8	22 ± 5	197 ± 36	1975
45	12.1	57 ± 18	129 ± 38	1304
67.5	10.4	85 ± 9	229 ± 49	2275

conclude that adsorption occurs. For anisaldehyde concentrations of 22.5 ppm and higher, the differential double-layer capacitance C_d does not change indicating a high degree of surface coverage. The most interesting parameter in Table 9 is the charge-transfer resistance R_F. For increasing values of the concentration of anisaldehyde an increased passivation of the lead oxidation process occurs.

From the adsorption isotherm of anisaldehyde at Cu, it was found before that at a concentration of ~ 20 ppm, coverage of Cu is completely. From Table 9 we conclude that at this concentration of anisaldehyde the passivation of Pb is restricted and does not lead to a disturbance of the Pb oxidation process and can therefore be used safely.

Discussion and conclusions

In this work a procedure is proposed for the selection of additives to be applied in lead/acid cells. The additives investigated were inhibitors for the HER and expanders for the negative plate.

The selection of inhibitors was done by d.c. and a.c. measurements at pure metals. These metals (Cu, Sb, and Ag) are considered to act as active sites for the HER at the negative plate. From this study, anisaldehyde was selected because of its preferential adsorption at Cu and Sb. In part 2 of this series tests of anisaldehyde in 2 V cells will be discussed [1].

The selection of expanders was done by means of impedance measurements using a Pb electrode discharged at a low anodic current density. From these measurements three physical parameters were obtained: the differential double-layer capacitance, C_d, the crystallization resistance, R_k and the Warburg impedance, A. A maximum was found for the value of R_k varying the concentration of the expander (Na-1-naphtol-4-sulfonate). This maximum in R_k corresponds to a minimum in the rate constant k for the formation of lead sulfate. For this minimum value of k the largest increase in charge and discharge capacity is found due to the formation of smaller size of lead sulfate crystals. From the analysis performed it was concluded that, for the expanders studied, the charge-transfer resistance, R_F, could be neglected. In the case of anisaldehyde added, it was shown that at higher concentrations (weak) passivation of Pb occurred ($R_F > 0$).

The influence of anisaldehyde on the discharge process of lead to lead sulfate was studied using a.c. impedance measurements. From this study it was found that for a concentration of 20 ppm of anisaldehyde no negative influence is found on the discharge process. At higher concentrations of anisaldehyde, passivation of lead occurs.

Especially short-time impedance measurements, which can be performed with high accuracy, are valuable both for selecting expanders and for enlarging the physical insight of the action (support of this is given in part 2, [1]).

Measurements in this study were conducted at room temperature. However, at practical conditions, large variations in temperature exist. In part 2, therefore, some attention will be paid to the influence of the temperature on inhibitor properties [1].

Acknowledgements

The authors wish to express their gratitude to Messrs H.E. Wijers, B. van de Ploeg and C. Posthumus of the Royal Netherlands Navy for their stimulating contributions to the project. We further acknowledge the Royal Netherlands Navy, TNO Defence Research and TNO Environmental and Energy Research for their financial support. The work was carried out under contract nr. A81/KM/074.

List of symbols

A	Warburg impedance, Ω cm^2 s$^{-1/2}$
c_0	equilibrium concentration of lead sulfate, mol cm^{-3}
C_d	differential double-layer capacity, μF cm^{-2}
C_d^0	differential double-layer capacity at zero coverage, μF cm^{-2}
C_d^1	differential double-layer capacity at unity coverage, μF cm^{-2}
E	potential versus reference electrode, V
i_{dc}	direct current density, mA cm^{-2}
j	imaginary unity
R_k	crystallization resistance, Ω cm^2
R_F	charge-transfer resistance, Ω cm^2
R_Ω	ohmic resistance, Ω cm^2
x	dimensionless parameter, $x = R_k\omega^{1/2}\sqrt{2}/A$
Y_e	electrode admittance, Ω^{-1} cm^{-2}
Y_e'	real part of electrode admittance, Ω^{-1} cm^{-2}
Y_e''	imaginary part of electrode admittance, Ω^{-1} cm^{-2}
Z'	real part of impedance, Ω cm^2
Z''	imaginary part of impedance, Ω cm^2
θ	partial surface coverage
ω	angular frequency, rad s^{-1}

References

1 M. Saakes, P.J. van Duin, A.C.P. Ligtvoet and D. Schmal, *J. Power Sources, 46* (1993) 149–158.
2 H. Döring, M. Radwan, H. Dietz, J. Garche and K. Wiesener, *J. Power Sources, 28* (1989) 381–396.
3 J.J. Mcmullen and N. Hackermann, *J. Electrochem. Soc., 106* (1959) 34.
4 E.V. Pashikova, M.A. Dasoyan, I.A. Aguf and M.L. Ratner, *Elektrotekhnica, 12* (1963) 41–45.
5 G. Hoffmann and W. Vielstich, *J. Electroanal. Chem., 180* (1984) 565.
6 K. Ledjeff, VARTA Batterie AG, *Ger. Patent No. 0 092 604* (Nov. 30, 1982).
7 M.P.J. Brennan and N.A. Hampson, *J. Electroanal. Chem., 52* (1974) 1.

8 D. Simonssen, P. Ekdunge and M. Lindgren, *J. Electrochem. Soc., 135* (1988) 1613.
9 E.M. Strochkova, K.V. Rybalka and D.I Leikis, *Sov. Electrochem., 11* (1975) 1355.
10 E.M. Strochkova and K.V. Rybalka, *Sov. Electrochem., 13* (1977) 62.
11 K.V. Rybalka and E.M. Strochkova, *Sov. Electrochem., 13* (1977) 1148.
12 V.S. Shaldaev and K.V. Rybalka, *Sov. Electrochem., 15* (1979) 323.
13 K.V. Rybalka and V.S. Shaldaev, *Sov. Electrochem., 17* (1981) 1375.
14 V.S. Shaldaev and K.V. Rybalka, *Sov. Electrochem., 13* (1977) 223.
15 B.K. Mahato, *J. Electrochem. Soc., 127* (1980) 1679.
16 B.K. Mahato, *J. Electrochem. Soc., 128* (1981) 1416.
17 VARTA Batterie AG, *Ger. Patent No. DT 2725-678* (June 6, 1977).
18 K.J. Vetter, *Elektrochemische Kinetik*, Springer, Berlin, 1961.
19 S. Gust, E. Hämeenoja, J. Ahl, T. Laitinen, A. Savonen and G. Sundholm, *J. Power Sources, 30* (1990) 185–192.
20 W. Simon, *Bosch Tech. Berichte, 1-Heft 5* (1966) 234–41.
21 P. Ruetschi, *US Patent No. 2 994 626* (1961).
22 D. Schmal and A.M.C.P. de Jong, *18th Int. Power Sources Symp., Stratford-on-Avon, UK, Apr. 19–21, 1993*, p. 33–41.
23 B.N. Kabanov, K.V. Rybalka and V.S. Shaldaev, *Sov. Electrochem., 14* (1978) 673–676.
24 K.V. Rybalka and M. Etman, *J. Electroanal. Chem., 148* (1983) 73–78.

Appendix

In the case where the charge-transfer resistance, R_F, can not be neglected, eqns. (2) and (3) are no longer valid. With R_F present, we have a total number of four parameters (R_F, R_k, C_d and A) which makes an analysis rather cumbersome. However, by introducing the dimensionless parameter $x=\sqrt{2R_k\omega^{1/2}}/A$ and by rearrangement of the expression for the electrode admittance Y_e given by (j = imaginary unity):

$$Y_e = j\omega C_d + \frac{1}{R_F + \dfrac{A}{A/R_k + (j\omega)^{1/2}}} \tag{A1}$$

to

$$\frac{1}{Y_e' + j(Y_e'' - \omega C_d)} = R_F + \frac{A}{A/R_k + (j\omega)^{1/2}} \tag{A2}$$

two linear equations are obtained by separating the real and imaginary part of eqn. (A2):

$$\frac{Y_e'}{(Y_e')^2 + (Y_e'' - \omega C_d)^2} = R_F + R_k \frac{2+x}{2+2x+x^2} \tag{A3}$$

and

$$\frac{Y_e'' - \omega C_d}{(Y_e')^2 + (Y_e'' - \omega C_d)^2} = R_k \frac{x}{2+2x+x^2} \tag{A4}$$

In eqn. (A1) the equality $j^{1/2} = (1+j)/\sqrt{2}$ was used. With a fixed value of C_d, it is easy to find x using a one-parameter optimalization (essentially R_k/A is taken as parameter). Subsequently, the values of R_F and R_k are obtained. The fitting criterion found most adequate was to bring both correlation coefficients of eqns. (A3) and (A4) as close to unity as possible. The internal consistency checks of this novel analysis method are three-fold:

- both slopes of eqns. (A3) and (A4) must be identical
- the intercept of eqn. (A3) must be larger than or equal to zero
- the intercept of eqn. (A4) must be zero

The best fit corresponds to those values of C_d and x which give the least value for the sum of squares of the differences between the experimental and theoretical values of Z' and Z''.